JMEPEG (2012) 21:1260–1265
DOI: 10.1007/s11665-011-0017-y

1059-9495/$19.00

Fracture Toughness of Friction Stir-Welded Lap Joints of Aluminum Alloys

M. Kemal Kulekci, Ibrahim Sevim, and Ugur Esme

(Submitted March 22, 2011; in revised form June 16, 2011)

The aim of this study is to determine the fracture toughness of friction stir-welded (FSW) lap joints of aluminum alloys. FSW lap joints of AA 2014 and AA 6063 aluminum alloy plates were performed on a conventional semiautomatic milling machine. FSW lap joints were produced on alloy plates. Fracture toughness of FSW lap joints were calculated from the results of tensile shearing tests. New empirical equations were developed for fracture toughness and energy release rate based on the relation between the hardness and fracture toughness values. Fracture toughness of FSW lap joints increases exponentially as the hardness reduces. The results of the experiments showed that the amount of Si content in Al alloys affects the fracture toughness of the FSW lap joints.

Keywords fatigue, fracture toughness, friction stir welding, friction welding

1. Introduction

Friction stir welding (FSW) offers a new, low-cost alternative to fusion welding procedures due to the low power requirements (Ref 1-3). Aluminum alloys with good heat transfer, high strength, good formability, and weight saving are being used for aerospace structure, shipbuilding, railway cars, etc. (Ref 4). The specific properties that affect the welding of aluminum and its alloys are its oxide characteristics, the solubility of hydrogen in molten aluminum, its thermal, electrical and non-magnetic characteristics, its alloys' wide range of mechanical properties and melting point (Ref 5-8).

In the FSW process, the strength of the metal of the interface between the rotating tool and workpiece, falls below the applied shear stress as the temperature rises, so that plasticized material is extruded from the leading side to the trailing side of the tool. The tool is then steadily moved along the joint line giving a continuous weld (Ref 9, 10). The plates to be welded are secured to prevent the butted joint faces from being forced apart as the pin tool passes through and along the seam. The heat-affected zone is much wider at top surface (in contact with shoulder) and tapers down (Ref 11).

Materials develop plastic strains as the yield stress is exceeded in the region near the crack tip (Ref 12). The amount of plastic deformation is restricted by the surrounding material, which remains elastic. The size of the created plastic zone depends on the stress conditions of the structure. If the stress intensity factor reaches a critical value K_c, unstable fracture occurs. The fracture toughness of a material is characterized by the energy per unit area, which is required to create new crack surfaces, and thereby propagate a crack through the material. The fracture toughness is dependent on specimen geometry, microstructure, phase composition, and temperature. This critical value of the stress intensity factor K_c is known as the fracture toughness of the material. Basic fracture modes are shown in Fig. 1. The fracture of a material is studied in three different modes (Ref 11). These are opening mode K_I, shearing mode K_{II}, and tearing mode K_{III}, as seen on Fig. 1.

The most widely used method for lap welds was recommended by Pook as, shearing mode K_{II} (Ref 12). K_{II} mode is used for lap welds in fracture toughness calculation (Ref 13). The fracture toughness of the FSW lap joints according to Mode II was calculated from the following equation, using the shearing tests and hardness tests results:

$$K_{II} = \tau\left(\pi\frac{D}{2}\right)^{1/2}\left[0.5 + 0.287\left(\frac{D}{t}\right)^{0.710}\right] \text{ (MPa m}^{1/2}\text{)} \quad \text{(Eq 1)}$$

where τ is the shear stress, D is the welding diameter (see Fig. 4 and 5), and t is the sheet thickness.

The strain energy release rate GII for Mode II is given by the following equation (Ref 13):

$$G_{II} = \frac{K_{II}^2\,(1-\nu^2)}{E} \text{ (MPa m)} \quad \text{(Eq 2)}$$

where ν is the Poisson ratio which is approximately 0.345, and E is the Young's modulus for aluminum alloys.

The previous research works are focused on the mechanical properties of FSW. However, there are limited studies for investigating the fracture toughness of FSW joints. Lack of comprehensive study for assessing the fracture toughness of FSW joints has led to this study to be carried out. This study focused on the fracture toughness of FSW lap joints. Similar

M. Kemal Kulekci and **Ugur Esme**, Department of Mechanical Education, Tarsus Technical Education Faculty, Mersin University, 33480 Tarsus, Turkey; and **Ibrahim Sevim**, Department of Mechanical Engineering, Engineering Faculty, Mersin University, 33343 Ciftlikkoy, Mersin, Turkey. Contact e-mails: uguresme@gmail.com and uesme2003@hotmail.com.

and dissimilar Al alloys were studied to investigate the fracture performance of FSW weld joints.

2. Experimental Studies

Commercial AA 2014 and AA 6063 aluminum alloy materials were used in this study. The thicknesses of these aluminum alloy plates were 4.35 mm for AA 2014 and 5.44 mm for AA 6063. The plates were machined out in 200 mm lengths and 100 mm widths. The composition and mechanical properties of the workpiece material are listed in Table 1 and 2 respectively.

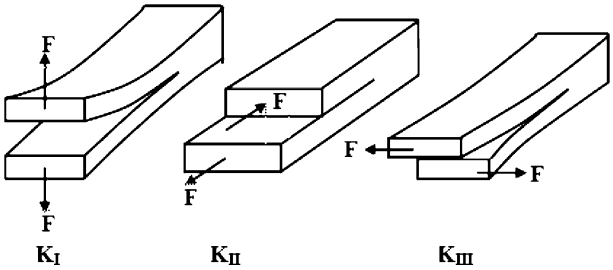

Fig. 1 Basic fracture modes: K_I: opening mode; K_{II}: shearing mode; K_{III}: tearing mode (Ref 3, 10)

Table 1 Chemical composition (wt.%) of aluminum alloys

	Al	Mg	Si	Mn	Zn	Fe	Ti	Cu	Cr	Sn
AA 2014	Balance	0.68	0.83	0.58	···	0.24	···	4.4	0.04	0.03
AA 6063	Balance	0.7	0.4	0.1	0.1	0.35	0.1	0.1	0.1	···

Table 2 Mechanical properties of aluminum alloys

Workpiece material	Yield strength, MPa	Ultimate tensile strength, MPa	Relative elongation, %	Hardness, HV
AA 2014	360	410	7	105
AA 6063	130	170	8	26

The shoulder diameter and threaded pin height of the tool were 15 and 6 mm, respectively. The diameter of the threaded pin was 5 mm (M5 screw). The shoulder was formed as a strait surface. Schematic illustration of the FSW tool and lap joint application, which was used in this study, is shown in Fig. 2.

The premachined plates were fixed rigidly on the table of the vertical semiautomatic milling machine for lap joint FSW as seen in Fig. 2(a) and 2(b). Then, tool was moved along the joint line. All of the FSW lap joints were obtained with 1200 rpm tool rotation and 60 mm/min traverse speed. Lap joints were welded as AA 2014 + AA 2014, AA 6063 + AA 6063, and AA 6063 + AA 2014 combinations. Ten shearing samples were extracted from the lap-welded plates.

Fracture toughness of FSW lap joints were calculated from the results of tensile shearing tests. A special tensile shearing test device was designed as seen in Fig. 3(a) and 3(b) and manufactured to perform tensile shearing tests on FSW lap joints.

The dimensions of the tensile shearing test specimens that were machined from the FSW lap-welded joints are shown in Fig. 4 and 5. The surface of the weld was cleaned by milling. The thicknesses of aluminum alloy plates used in the study were 4.35 mm (t1), for AA 2014 and 5.44 mm (t2) for AA 6063. D is the diameter of the pin (M5 = 5 mm).

Hardness of FSW joints were measured on the weld center of sheared surfaces after tensile shearing tests. The sheared surfaces were polished with 200-1000 grit abrasive paper and etched using Keller's etch, then the hardness was measured with Vickers hardness tester using 1.96 N ($HV_{0.2}$). The metal of the welded plates is stirred up at the interface of the plates. Stirring of two different metal alloys caused hardness differences at the joint interface. Hardness difference can be explained with the different stirring effect between advancing side and retreating side of welding. Hardness values measured on the sheared surfaces of joints are shown in Fig. 6-8.

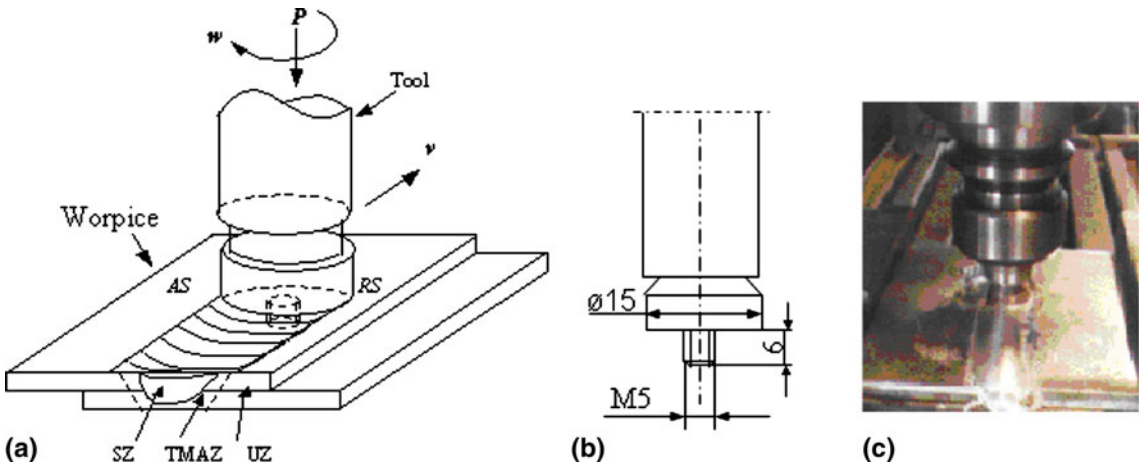

Fig. 2 Schematic illustration of FSW lap joints and FSW application on conventional vertical milling machine. (a) Schematic illustration of FSW lap joints performed in the study (SZ: stirring zone, TMAZ: thermo-mechanically affected zone—transition zone, UZ: unaffected zone—base metal, AS: advancing side, RS: retreating side), (b) dimensions of the FSW tool, and (c) FSW application on conventional vertical milling machine and fixed plates

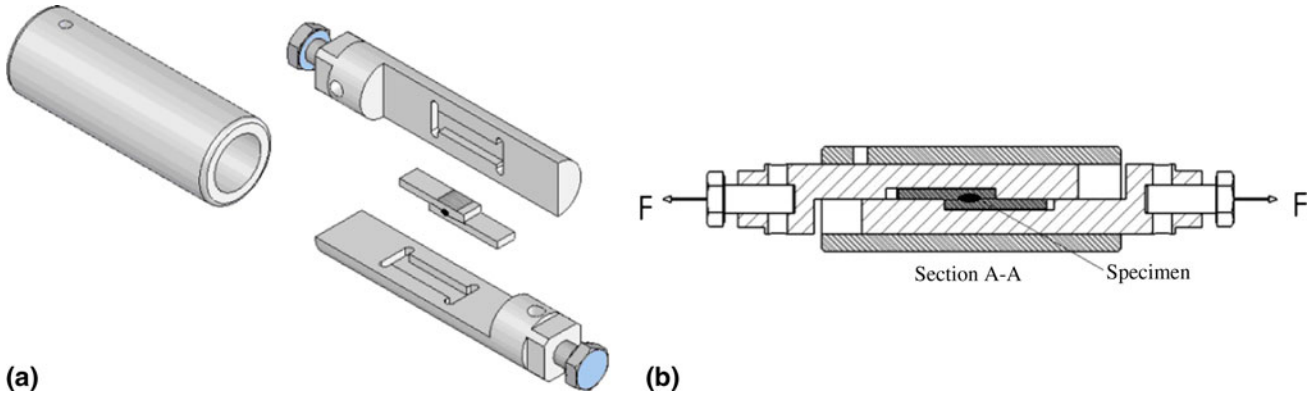

Fig. 3 Tensile shearing test device. (a) Three-dimensional model and (b) sectional view of tensile shearing test device

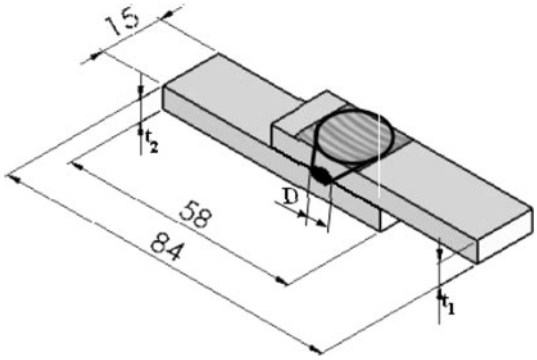

Fig. 4 Lap-welded joint specimen (The thicknesses of aluminum alloy plates used in the study were 4.35 mm (t1), for AA 2014 and 5.44 mm (t2) for AA 6063. *D* is the diameter of the pin (M5 = 5 mm))

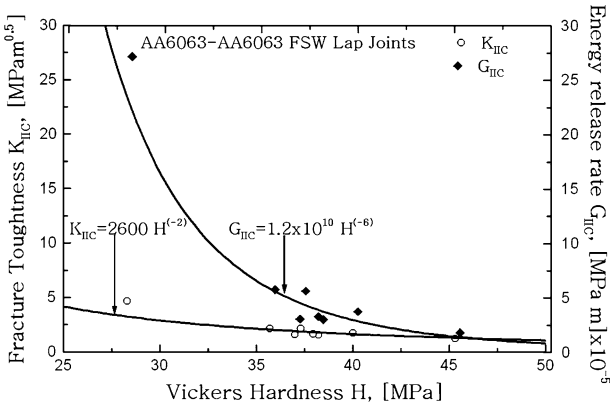

Fig. 6 Fracture toughness variation with hardness in FSW lap joints of AA 6063-6063

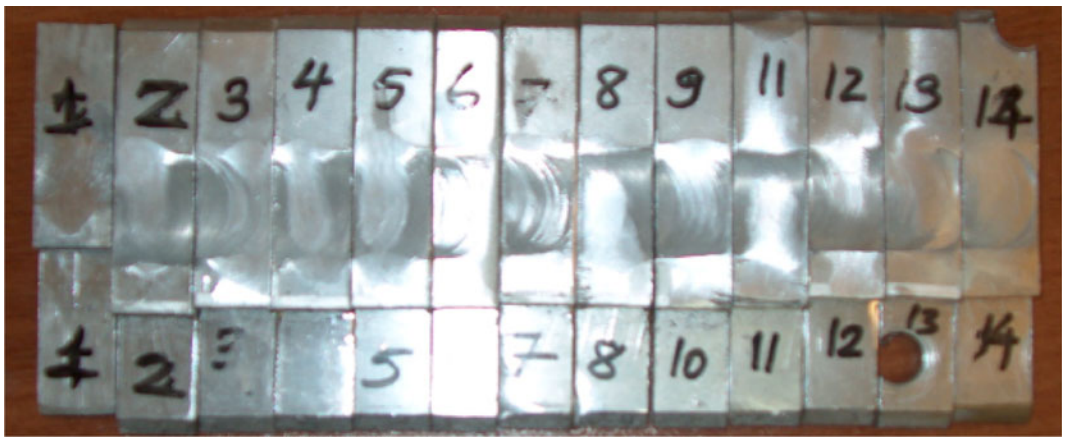

Fig. 5 Tensile shearing test samples machined out from FSW lap joints. All of the FSW lap joints were obtained with 1200 rpm tool rotation and 60 mm/min traverse speed (samples numbered 1, 2, 3, and 4 are from AA 2014 + AA 2014; samples numbered 5, 6, 7, 8, and 9 are from AA 6063 + AA 6063 and samples numbered 11, 12, 13, and 14 are from AA 6063 + AA 2014 combinations)

3. Results

The fracture toughness value (K_{IIC}), and the strain energy release rate (G_{IIC}) were computed for FSW sheets applying the Eq 1, and 2, respectively. The variation of K_{IIC} and G_{IIC} with the Vickers hardness $HV_{0.2}$ measured on the sheared surface is shown in Fig. 6-8. The metal of the welded plates is stirred up at the interface of the plates. This situation explains that the stirring of the metal at the interface of the two plates affects the hardness of the stirred metal.

The fracture toughness and the strain energy release rate decrease with increasing Vickers Hardness is shown in Fig. 6-11.

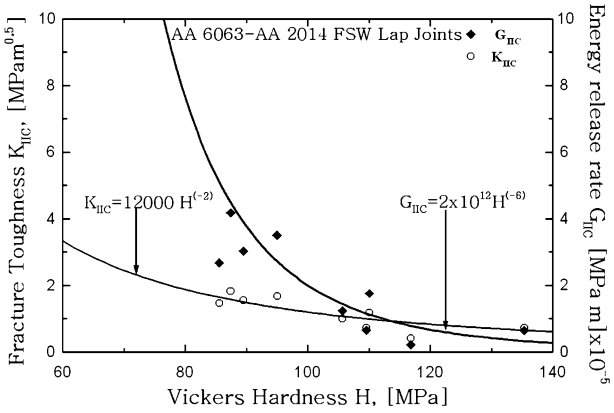

Fig. 7 Fracture toughness variation with hardness in FSW lap joints of AA 6063-2014

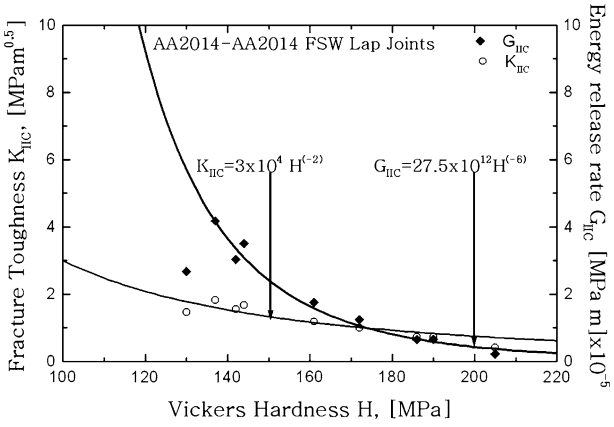

Fig. 8 Fracture toughness variation with hardness in FSW lap joints of AA 2014-2014

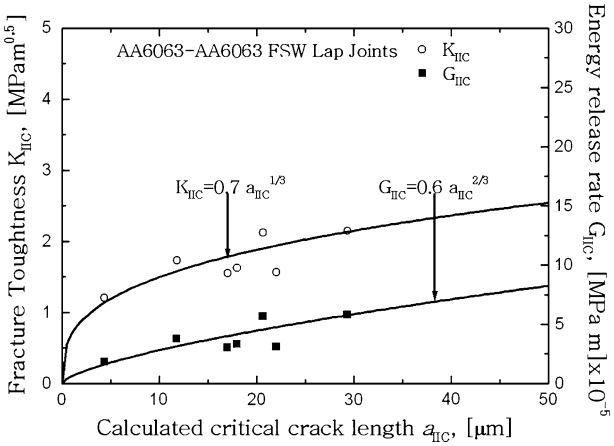

Fig. 9 Fracture toughness variation with calculated critical crack length in FSW lap joints of AA 6063-6063

The decrease is proportional to H^{-2} and H^{-6} for fracture toughness value and the strain energy release rate, respectively.

We developed the following relation between fracture toughness and hardness of FSW of the materials studied using the least squares method of curve fitting (Fig. 6-8).

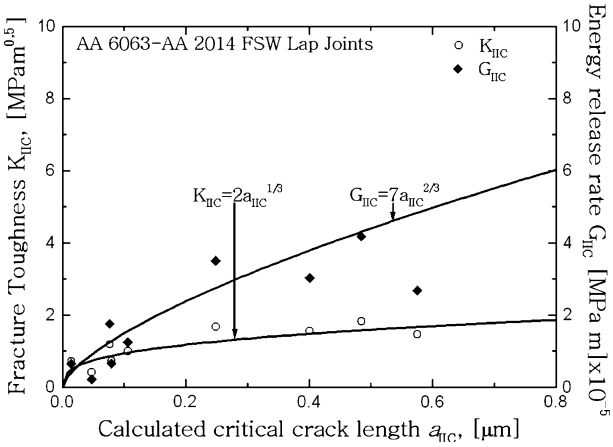

Fig. 10 Fracture toughness variation with calculated critical crack length in FSW lap joints of AA 6063-2014

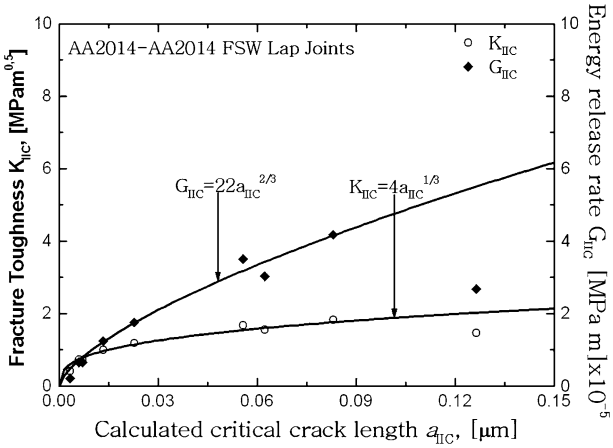

Fig. 11 Fracture toughness variation with calculated critical crack length in FSW lap joints of AA 2014-2014

$$K_{IIC} = 2600H^{-2} \quad \text{for AA6063-60063} \qquad \text{(Eq 3a)}$$

$$K_{IIC} = 12000H^{-2} \quad \text{for AA6063-2014} \qquad \text{(Eq 3b)}$$

$$K_{IIC} = 30000H^{-2} \quad \text{for AA2014-2014} \qquad \text{(Eq 3c)}$$

where K_{IIC} is fracture toughness for Mode II (MPa $m^{1/2}$) and H is Vickers hardness (MPa).

Effect of cracks on fracture can be expressed by the inequality

$$K_{II} \geq K_{IIC}. \qquad \text{(Eq 4)}$$

The following expression for K_{II} was modified from the relation in the literature (Ref 14) for this study to compute the critical crack lengths:

$$K_{II} = \tau\sqrt{\pi a_{IIC}} \qquad \text{(Eq 5)}$$

where τ is the applied shear stress and a_{IIC} is the critical crack length.

The plastic deformation can be expressed as

$$\tau \cong \tau_{yield} \qquad \text{(Eq 6)}$$

and

$$\tau_{yield} = \frac{\sigma_{yield}}{2} \qquad \text{(Eq 7)}$$

The relation between the hardness and yield stress can be defined (Ref 14) as

$$H \cong 3\sigma_{yield} \quad \text{(Eq 8)}$$

and by using Eq 8, the following equations can be obtained for stress intensity factors:

$$K_{II} = \frac{H}{6}\sqrt{\pi a_{IIC}} \quad \text{(Eq 9)}$$

Substituting (9) into (3a), the following equations are obtained:

$$\frac{H}{6}\sqrt{\pi a_{IIC}} \geq 2600H^{-2} \quad \text{(Eq 10a)}$$

$$\frac{H}{6}\sqrt{\pi a_{IIC}} \geq 12000H^{-2} \quad \text{(Eq 10b)}$$

$$\frac{H}{6}\sqrt{\pi a_{IIC}} \geq 30000H^{-2} \quad \text{(Eq 10c)}$$

Equation 10a, 10b, and 10c were used for AA 6063-6063, AA 6063-AA 2014, and AA 2014-2014 FS weld joints, respectively.

Rearranging (10a, 10b, and 10c), the critical crack length, a_{IIC}, can be expressed as

$$a_{IIC} \geq \frac{36}{\pi}\left(\frac{2600}{H^4}\right)^2 \quad \text{(Eq 11a)}$$

$$a_{IIC} \geq \frac{36}{\pi}\left(\frac{12000}{H^4}\right)^2 \quad \text{(Eq 11b)}$$

$$a_{IIC} \geq \frac{36}{\pi}\left(\frac{30000}{H^4}\right)^2 \quad \text{(Eq 11c)}$$

The variation of the critical crack lengths that are calculated in Eq 11a, 11b, and 11c is shown in Fig. 9-11. It is clear from Fig. 9-11 and Eq 11a, 11b, and 11c that the critical crack length becomes smaller as the hardness increases.

Fracture toughness values can be calculated by using the following equation:

$$K_{IIC} = 0.7a_{IIC}^{1/3} \quad \text{(Eq 12a)}$$

$$K_{IIC} = 2a_{IIC}^{1/3} \quad \text{(Eq 12b)}$$

$$K_{IIC} = 4a_{IIC}^{1/3} \quad \text{(Eq 12c)}$$

Fracture toughness values obtained from the Eq 12a, 12b, and 12c are shown in Fig. 9-11.

The critical crack length versus the strain energy release rate (G_{IIC}), which was calculated by using Eq 2 is shown in Fig. 9-11.

Figure 9-11 shows that the increase in critical crack length is proportional to the (2/3) of the strain energy release rate (G_{IIC}) values.

4. Discussion

Fracture toughness of FSW lap joints are shown in Fig. 6-8. From these figures, it is clear that the fracture toughness of FSW lap joints increases exponentially as the hardness reduces.

Figure 6-8 shows that the FSW lap joints which have lower hardness value have higher fracture toughness. From these figures, it is seen that the fracture toughness of FSW lap joints of AA 2014-2014 is higher from the joints of AA-6063-6063. This situation can be explained with the hardness difference between AA 2014 and AA 6063. Chung et al. states in their study that recrystallization results in finer grain size. The hardness of the finer grain size is higher than the base metal (Ref 15).

Critical crack length of FSW welds, which is calculated from Eq 10a, 10b, and 10c is shortened when hardness is increased. Shortening of critical crack length, lowers fracture toughness value. Critical cracks in the weld zone may cause microcracks or segregation-induced fracture. Fracture intensity factor in the welding zone varies with the root square of critical crack length. These values are resulted from segregations, grain boundaries, microporosity, and capillary cracks. Fracture toughness of the weld zone changes inversely proportional with the hardness (Ref 16-18). The metal of the welded plates is stirred up at the interface of the plates as seen in Fig. 6-8. From these figures, it is seen that the fracture toughness values of the AA 6063-AA 2014 joints were resulted between the joints of AA 6063-6063 and AA 2014-2014. This situation explains that the stirring of the metal at the interface of the two plates affects the fracture toughness of the lap joints.

5. Conclusions

In this study, fracture toughness of FSW lap joints were calculated from the results of tensile shearing tests. New empirical equations were developed for fracture toughness and energy release rate based on the relation between the hardness and fracture toughness values. The following conclusions can be drawn from this study:

- Fracture toughness of FSW lap joints increases exponentially as the hardness of the weld is reduced.
- The amount of Si alloy element affects the fracture toughness of the FSW lap joints.
- Increase in the Si ratio in Al alloy reduces the fracture toughness.
- Stirring of the materials at the interface of welded plates affects the fracture toughness of lap joints.
- There is a relationship between fracture toughness and calculated critical crack length in FSW lap joints. Shortening of critical crack length, lowers fracture toughness value.
- Stirring effect of FSW process results in finer grain sizes and higher hardness value.
- Critical crack length, which causes fracture of FSW lap joints, shortens as the hardness of the weld increases.

Acknowledgments

This study is supported by "Research Foundation of Mersin University" under project of 2007/2.

References

1. S.R. Ren, Z.Y. Ma, and L.Q. Chen, Effect of Welding Parameters on Tensile Properties and Fracture Behavior of Friction Stir Welded Al-Mg-Si Alloy, *Scr. Mater.*, 2007, **56**(1), p 69–72

2. G. Çam, H.T. Serindağ, A. Çakan, S. Mıstıkoğlu, and H. Yavuz, The Effect of Weld Parameters on Friction Stir Welding of Brass Plates, *Mat.-wiss. u. Werkstofftech.*, 2008, **39**(6), p 394–399
3. M.K. Kulekci, F. Mendi, I. Sevim, and O. Basturk, Fracture Toughness of Friction Stir-Welded Joints of $AlCu_4SiMg$ Aluminium Alloy, *Metalurgija*, 2005, **44**(3), p 209–213
4. G. Çam, S. Güçlüer, A. Çakan, and H.T. Serindağ, Mechanical Properties of Friction Stir Butt-Welded Al-5086 H32 Plate, *Mat.-wiss. u. Werkstofftech.*, 2009, **40**(8), p 638–642
5. H. Uzun, C.D. Donne, A. Argagnotto, T. Ghidini, and C. Gambaro, Friction Stir Welding of Dissimilar Al 6013-T4 To X5CrNi18-10 Stainless Steel, *Mater. Des.*, 2005, **26**(1), p 41–46
6. S. Rajakumar, C. Muralidharan, and V. Balasubramanian, Influence of Friction Stir Welding Process and Tool Parameters on Strength Properties of AA7075-T-6 Aluminium Alloy Joints, *Mater. Des.*, 2010, **32**(2), p 535–539
7. K. Colligan, Material Flow Behaviour During Friction Stir Welding of Aluminium, *Weld. Res.*, 1999, **78**(7), p 229–237
8. M.K. Kulekci and A. Sik, Effects of Tool Rotation and Traverse Speed on Fatigue Properties of Friction Stir Welded AA 1050-H18 Aluminium Alloy, *Arch. Metall. Mater.*, 2006, **51**(2), p 213–216
9. J.Q. Su, T.W. Nelson, R. Mishra, and M. Mahoney, Microstructural Investigation of Friction Stir Welded 7050-T651 Aluminium, *Acta Mater.*, 2003, **51**(3), p 713
10. M.K. Kulekci, E. Kaluc, A. Sik, and O. Basturk, Experimental Comparison of MIG and Friction Stir Welding Processes for En AW-6061-T6 (Al Mg-1 Si Cu) Aluminium Alloy, *Arab. J. Sci. Eng.*, 2010, **35**(1B), p 321–330
11. W.M. Thomas, K.I. Johnson, and C.S. Wiesner, Friction Stir Welding—Recent Developments in Tool and Process Technologies, *Adv. Eng. Mater.*, 2003, **5**(7), p 485–490
12. I. Sevim and B. Eryürek, Effect of Fracture Toughness on Abrasive Wear Resistance of Steels, *Mater. Des.*, 2006, **27**(10), p 911–919
13. D. Broek, *Elementary Engineering Fracture Mechanics*, Noordhoff International Publishing, Neyden, The Netherlands, 1976
14. I. Sevim, Fracture Toughness for Spot-Welded Steel Joints, *Kovove Mater.*, 2005, **43**(2), p 113–123
15. Y.D. Chung, H. Fujii, K. Nakata, and K. Nogi, Friction Stir Welding of High Carbon Tool Steel (SK85) Below Eutoctoid Temperature, *Trans. JWRI*, 2009, **38**(1), p 37–41
16. ACA METAL, from http://www.acametal.com.tr/page.php?ID=17, Accessed on February 9, 2011
17. I. Sevim, Effect of Hardness to Fracture Toughness for Spot Welded Steel Sheets, *Mater. Des.*, 2006, **27**(1), p 21–30
18. G. Çam, S. Mistikoglu, and M. Pakdil, Microstructural and Mechanical Characterization of Friction Stir Butt Joint Welded 63% Cu-37% Zn Brass Plate, *Weld. J.*, 2007, **88**, p 225–232